

Michał DOBRZYŃSKI^{a,*}, Lubomir JAVOREK^b,
Kazimierz A. ORŁOWSKI^a, Włodzimierz PRZYBYLSKI^a

^a Faculty of Mechanical Engineering, Gdańsk University of Technology, Gdansk, Poland

^b Faculty of Environmental and Manufacturing Technology, Technical University in Zvolen, Zvolen, Slovak Republic

* Corresponding author: mdozbrzyn@pg.edu.pl

THE EFFECT OF AN ACTIVE FORCE WHILE SLIDE DIAMOND BURNISHING OF WOODEN SHAFTS UPON PROCESS QUALITY

© 2019 Michał Dobrzyński, Lubomir Javorek, Kazimierz A. Orłowski, Włodzimierz Przybylski

This is an open access article licensed under the Creative Commons Attribution International License (CC BY)



<https://creativecommons.org/licenses/by/4.0/>

Key words: wooden shaft, great maple, burnishing, surface quality, 3D surface texture.

Abstract: The quality of the surface of wooden elements that have been turned and burnished has got a crucial meaning in the whole production process flow, since the obtained effects affect the quality of the wooden surface after finishing (coating, painting). In the paper, selected results of the investigation of the effect of the burnishing process on the surface quality of the elements after turning are presented. Research experiments were conducted on a lathe with a slide diamond burnisher and active (loading) forces: 30 N, 50 N, and 70 N. The elements under treatment were of great maple (*Acer pseudoplatanus* L.). The following report presents measuring results of the surface layer condition as well as some profile samples, and dimensional and geometrical deviations analysis.

Wpływ siły czynnej podczas ślizgowego nagniatania diamentem wałków drewnianych na jakość obróbki

Słowa kluczowe: drewniane wałki, jawor, nagniatanie, jakość powierzchni, tekstura powierzchni.

Streszczenie: Jakość powierzchni elementów drewnianych, które zostały toczone i nagniatane, ma decydujące znaczenie w całym procesie produkcji, ponieważ uzyskane efekty wpływają na jakość drewnianych powierzchni po obróbce finalnej (pomalowaniu, malowaniu). W artykule przedstawiono wybrane wyniki badań wpływu procesu nagniatania na jakość powierzchni elementów po toczeniu. Eksperymenty badawcze przeprowadzono na tokarce diamentowym narzędziem nagniatającym dla sił: 30 N; 50 N i 70 N. Obrabiane elementy wykonane były z drewna jaworowego (*Acer pseudoplatanus* L.). Poniższy raport przedstawia wyniki pomiarów stanu warstwy wierzchniej, a także analizy wybranych profili, odchylek wymiarowych i geometrycznych.

Introduction

The surface of products after machining, e.g., turning or milling, are too rough and require expensive finishing. Moreover, the dimensional and surface qualities of solid wood products are the most important properties influencing further manufacturing processes, such as finishing (coating) [1, 2, 3, 4]. The high roughness is a result of an inaccurate shearing as well as cell wall deformations and other factors connected with heterogeneous wood structure. Sanded surfaces require many additional treatments before varnishing, dyeing,

painting, or wax coating. Besides several advantages, the sanding process has also many disadvantages such as the following: the process can gum the sandpaper up when sanding soft, resinous materials, which reduces tool life, the sanded surface could be burnt, and the working environment is contaminated by dust, which is often a danger to the staff. One of the alternative methods of wood surface finishing is a simultaneous application of load, heat, and friction between the tool and machined surface. The main goal of densifying sawn timber is to increase its hardness and surface abrasion resistance and, in some cases, also to increase its strength [5, 6]. Densifying sawn timber leads to a compression

of the wood cells throughout the entire volume of the sawn timber, coining the term “bulk densification.” An example of surface densification, which does not densify the entire volume, is presented in Fig. 1.

Past studies into surface densification of wood were aimed mainly at exploring different process approaches:

1. Thermorolling during continuous roller pressing of Scots pine boards at a process speed of up to 80 m min^{-1} [7]. In this technics the whole process of surface densification is a workflow consisting of dedicated stages, such as plasticisation, densification, solidification, and stabilization [5]. This manufacturing concept has also been tested with success in a conventional continuous MDF panel press [8].
2. Sliding smoothing with a ball shaped burnishing tool of round workpieces (shafts or balusters) on a lathe (Fig. 2). The process generates heat in the surface layer as a result of load and friction [9]. In this case, the pressure value should be higher than compression strength of the treated wood. The idea of this surface layer formation is shown in Fig. 2. In this process, thermo plastification is redundant.
3. Roller burnishing which has similar applications as sliding smoothing [10].
4. Ultrasonic smoothing – the tool has ultrasonic vibrations, which are transmitted to the machined surface, and they generate friction in the contact zone. The vibrating tool is perpendicular to the direction of the feed motion. The generated heat causes lignin softening and conglutination of torn wood grains with the machined surface [11, 12].
5. Treatment of the softened wood surface with friction and in the next step with load [13].

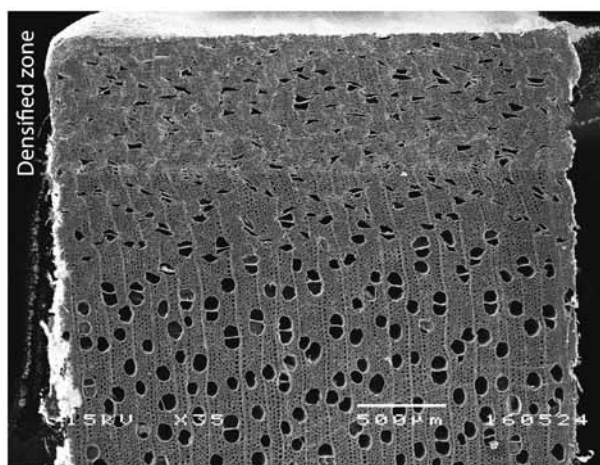


Fig. 1. Cross-section views of poplar (*Populus deltoides* Bartr. ex.) at $35\times$ magnification after surface densification showing cell deformation close to the surface

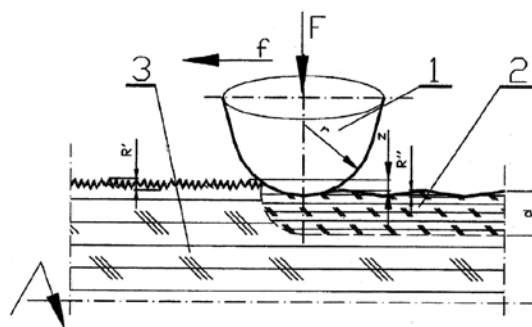


Fig. 2. The scheme of the surface layer formation by sliding burnishing of wood, where: 1 – burnishing tool, 2 – densified surface layer, 3 – sample core with undeformed structure (the entire volume), F – load (active) force, f – feeding direction, r – radius of spherical cup, R' , R'' – roughness profile heights

1. Materials and methods

The materials under investigation were in the form of wooden $\varnothing 52 \text{ mm}$ shaft made of great maple (*Acer pseudoplatanus* L.). The moisture content of the material was $\text{MC } 12\% \pm 2\%$. Turning and burnishing processes were carried out on the turning machine CU580H. In the research, a turning knife with the self-propelled turning insert of a special design was applied (Fig. 3a). The diameter of the high speed steel (HS10-0-4: PN-EN ISO 4957:2004) insert was $\varnothing 20 \text{ mm}$. The knife is also characterized by clearance angles $\alpha_f = 12^\circ$, rake angle $\gamma_f = 10^\circ$, and elevation setting angle $H = 20^\circ$. The woodworking parameters in the turning operation were established to the following: cutting depth $a_p = 2 \text{ mm}$, feed $f = 0.20 \text{ mm}$, and cutting speed $v_c = 200 \text{ m/min}$. The finishing machining using a slide diamond burnisher was conducted with a feed $f = 0.20 \text{ mm}$, a spindle rotational speed $n = 100 \text{ rpm}$, and an active (loading) force: 30 N (Sample#1); 50 N (Sample#2) and 70 N (Sample#3) (Fig. 3b).

The surface texture validations were carried out with the surface roughness tester Hommelwerk Standard 1000, according to the recommendations in the work [14]. During the measurements, the following parameters were adopted: evaluation length $l_n = 12.5 \text{ mm}$, cut off value $\lambda_c = 2.5 \text{ mm}$, cut off ratio $\lambda_c/\lambda_s = 300$, and sampling interval $1.5 \mu\text{m}$. The stylus end was conical (taper angle of cone 60°) with a spherical tip (tip radius $r_{\text{tip}} = 2 \mu\text{m}$). Additionally, the surface topography measurements of the selected parts were made with a 3D Optical Profiler S Neox with objective $10\times$ magnification (EPI 10x v35), topography 1354×1018 pixels, area $1746.66 \times 1313.22 \mu\text{m}$, pixel size $1.3 \mu\text{m/pixel}$, threshold 3%, and Confocal Fusion algorithm [15]. The measurements of dimensional and geometrical deviations were made on a Coordinated Measuring Machine Altera 7.5.5 Nikon

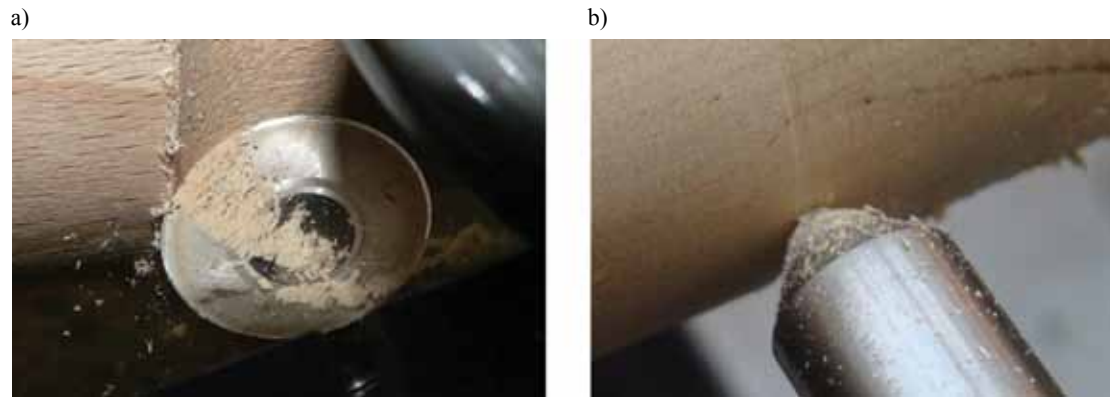


Fig. 3. Turning process with rotating blade knife (a) and slide diamond burnishing (b)

Metrology NV with the CMM Manager v. 3.6 software and probe system: PH10M PLUS + SP25M with probing $MPE_p = 1.6 \mu\text{m}$ according to ISO 10360-2:2009, length measurement $MPE_E = 1.8+L/400 \mu\text{m}$ according to ISO 10360-2:2009 and standard temperature range 18–22°C [16].

2. Results and discussion

The spread of diameters after the turning process was the largest, while further burnishing processing generally resulted in its reduction (Table 1). The largest dispersion reduction, more than four times, was

observed for Sample#1 when the loading force of the burnishing element on the machined surface was the smallest (30 N). A similar situation occurred for the designated circularity tolerances. However, the decrease of the roundness was greater, up to about 0.04 mm and 0.07 mm for Sample#1 and Sample#2, respectively, while the corresponding value of about 0.1 mm was obtained after the turning process (Fig. 4). Therefore, it can be concluded that increasing the burnishing loading force above 30 N causes an increase in both dimensional and geometric tolerances. At high loading forces of 70 N, reached values were similar to those obtained after turning machining.

Table 1. Main statistics of diameter and circularity deviations for samples under investigation

| Part after turning | | | | | |
|--------------------|---------------|------------------|----------------|----------------|---------------|
| | Diameter [mm] | Circularity [mm] | Max. Dev. [mm] | Min. Dev. [mm] | RMS Dev. [mm] |
| Spread | 0.135 | 0.114 | 0.053 | 0.062 | 0.043 |
| Mean | 48.216 | 0.097 | 0.047 | -0.050 | 0.036 |
| Median | 48.218 | 0.111 | 0.054 | -0.058 | 0.042 |
| Sample#1 | | | | | |
| | Diameter [mm] | Circularity [mm] | Max. Dev. [mm] | Min. Dev. [mm] | RMS Dev. [mm] |
| Spread | 0.032 | 0.026 | 0.017 | 0.009 | 0.010 |
| Mean | 47.914 | 0.036 | 0.019 | -0.016 | 0.013 |
| Median | 47.919 | 0.031 | 0.017 | -0.014 | 0.011 |
| Sample#2 | | | | | |
| | Diameter [mm] | Circularity [mm] | Max. Dev. [mm] | Min. Dev. [mm] | RMS Dev. [mm] |
| Spread | 0.134 | 0.036 | 0.006 | 0.030 | 0.016 |
| Mean | 47.878 | 0.067 | 0.027 | -0.040 | 0.025 |
| Median | 47.871 | 0.072 | 0.026 | -0.046 | 0.028 |
| Sample#3 | | | | | |
| | Diameter [mm] | Circularity [mm] | Max. Dev. [mm] | Min. Dev. [mm] | RMS Dev. [mm] |
| Spread | 0.099 | 0.023 | 0.013 | 0.011 | 0.008 |
| Mean | 47.667 | 0.094 | 0.037 | -0.057 | 0.037 |
| Median | 47.669 | 0.089 | 0.033 | -0.056 | 0.035 |

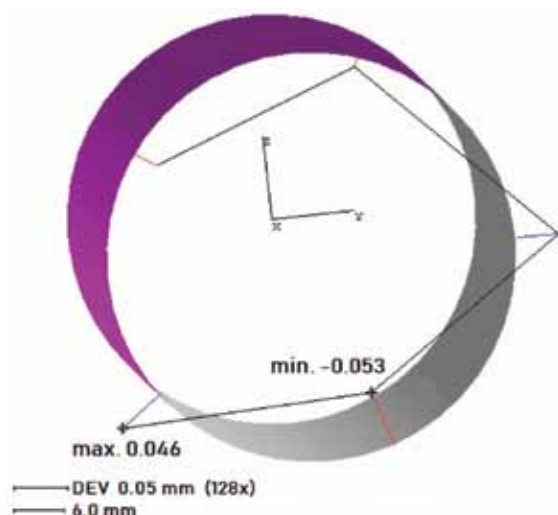


Fig. 4. Circularity deviations of the part after turning

In the cases under investigated, only the cylindricity errors were reduced, even for the burnished samples with a loading force of 70 N (Table 2). However, it should be emphasized that the length of turned samples were nearly four times greater and the obtained results cannot be directly compared (Fig. 5). At the burnishing loading forces of 30 N and 50 N, the cylindricity tolerances were about 0.01 and were 2.5 times lower than that for the highest force.

Table 2. Cylindricity deviations of the parts after investigation

| | Cylindricity [mm] | Max. Dev. [mm] | Min. Dev. [mm] | RMS Dev. [mm] |
|--------------------|-------------------|----------------|----------------|---------------|
| Part after turning | 0.509 | 0.221 | -0.288 | 0.145 |
| Sample#1 | 0.094 | 0.063 | -0.031 | 0.023 |
| Sample#2 | 0.097 | 0.051 | -0.046 | 0.032 |
| Sample#3 | 0.246 | 0.163 | -0.083 | 0.063 |

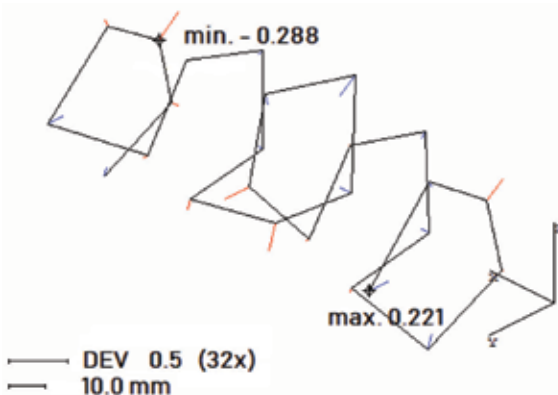


Fig. 5. Cylindricity deviations of the Part after turning

The irregularities of the parts after turning were evaluated applying mean parameters, such as root mean square height (R_q) and arithmetical mean height (R_a) (Table 3). Individual maximum and minimum height values observed have a larger effect on R_q values than on R_a . The mean and median differences reached 30% with a high dispersion of the results, as indicated by the maximum/minimum values and interquartile box (Fig. 6a). Such differences are characteristic for irregular profiles with deep valleys and high peaks, and they reflect the general texture of the turned surface having considered texture of the wood. Therefore, the mean and median of the total height of profile (R_t) amounted to almost $68 \mu\text{m}$, while lower quartile (Q_1) and upper quartile (Q_2) were $40.19 \mu\text{m}$ and $48.84 \mu\text{m}$ for the maximum height (R_z), respectively (Fig. 6b). Negative skewness R_{sk} in the range of $-1.45 - -0.07$ and mean/median of $-0.63/-0.65$ suggests that peaks after turning the wooden material were smooth, but surfaces were generally characterized by almost normal Gaussian distributions of ordinates.

Table 3. Roughness parameters of the parts after turning

| | R_a [μm] | R_q [μm] | R_z [μm] | R_t [μm] | R_{sk} |
|--------|-------------------------|-------------------------|-------------------------|-------------------------|----------|
| Mean | 7.14 | 9.48 | 44.67 | 65.65 | -0.63 |
| Median | 6.75 | 8.87 | 42.11 | 67.46 | -0.65 |
| Q_1 | 6.32 | 8.25 | 40.19 | 54.98 | -0.92 |
| Q_3 | 8.05 | 10.87 | 48.84 | 74.27 | -0.23 |
| Max | 8.43 | 11.53 | 55.45 | 85.07 | -0.07 |
| Min | 6.15 | 8.00 | 38.16 | 47.68 | -1.45 |

In most cases, the arithmetical mean height (R_a) for parts burnished with the loading force of 30N (Sample#1) were in the range of $3.39-5.54 \mu\text{m}$ at the mean value about $4.50 \mu\text{m}$ (A#1) (Table 4). However, areas with a worse surface during the tests were isolated (A#2). These surfaces were characterized by a higher R_a parameter of $4.5 \mu\text{m}$, and the total height of profile (R_t) amounted to almost $92 \mu\text{m}$ (Fig. 7). Selected 3D measurements confirmed the above findings. The root mean square heights (S_q) were in the range of $7.22-7.84 \mu\text{m}$,

Table 4. Roughness parameters of the parts burnished with the loading force of 30 N (Sample#1)

| | A#1 | | A#2 | |
|---------|-------------------------|-------------------------|-------------------------|-------------------------|
| | R_a [μm] | R_t [μm] | R_a [μm] | R_t [μm] |
| Mean | 4.56 | 45.15 | 7.96 | 72.15 |
| Median | 4.40 | 44.56 | 7.94 | 75.10 |
| Q_1 | 4.16 | 37.46 | 6.78 | 65.54 |
| Q_3 | 5.21 | 48.36 | 9.37 | 77.47 |
| Max | 5.54 | 53.67 | 9.90 | 91.97 |
| Min | 3.39 | 31.89 | 6.15 | 49.17 |
| Outlier | - | 70.47 | - | - |

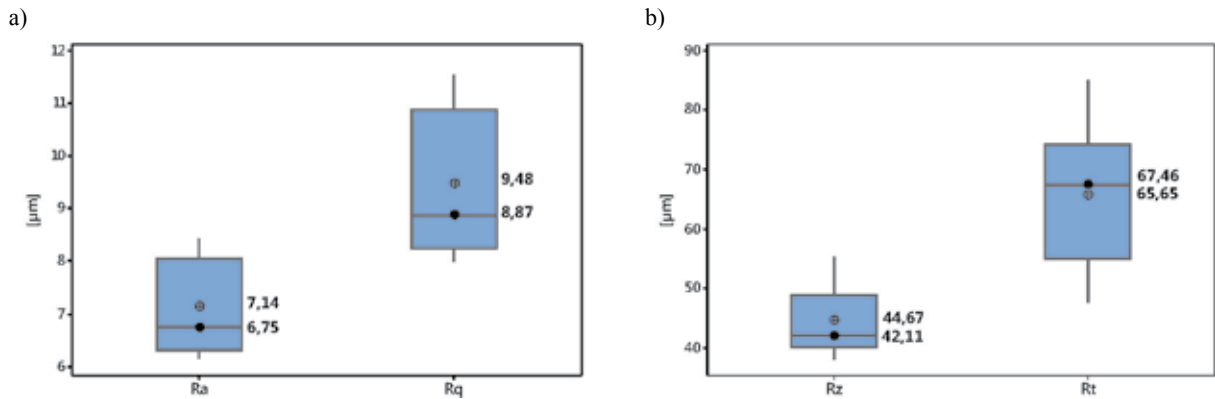


Fig. 6. The centre and spread of a Ra and Rq (a) and Rz and Rt (b) parameters of the profile (the box plot presents: the mean, the median, the interquartile range box and the range of the data)

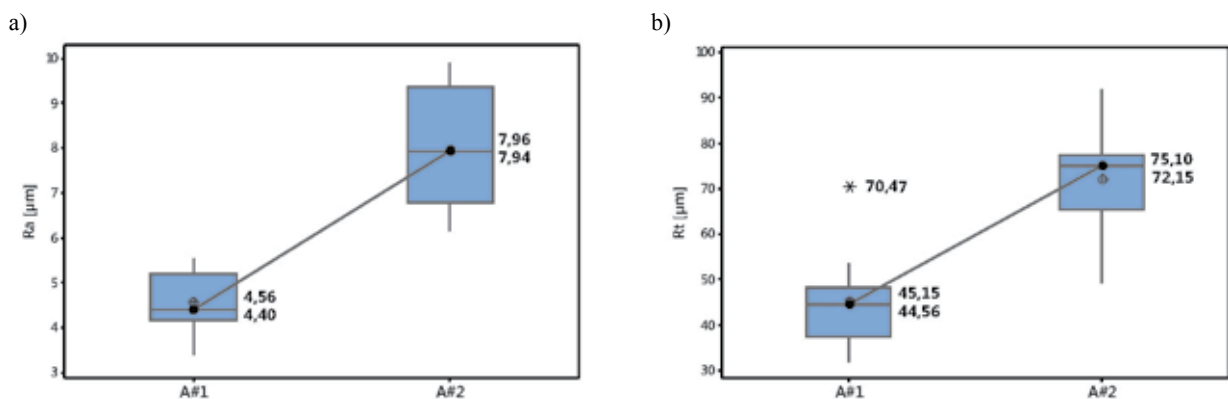


Fig. 7. The centre and spread of a Ra (a) and Rt (b) parameters of the profile of the parts burnished with the loading force of 30 N (Sample#1) (the box plot presents: the mean, the median, the interquartile range box and the range of the data)

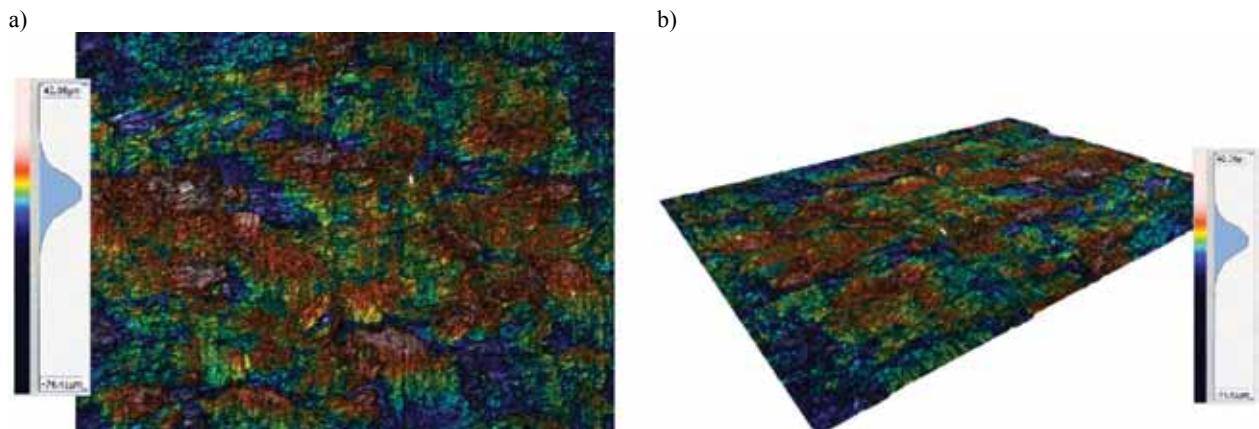


Fig. 8. Surface topography 2D (a) and 3D (b) view

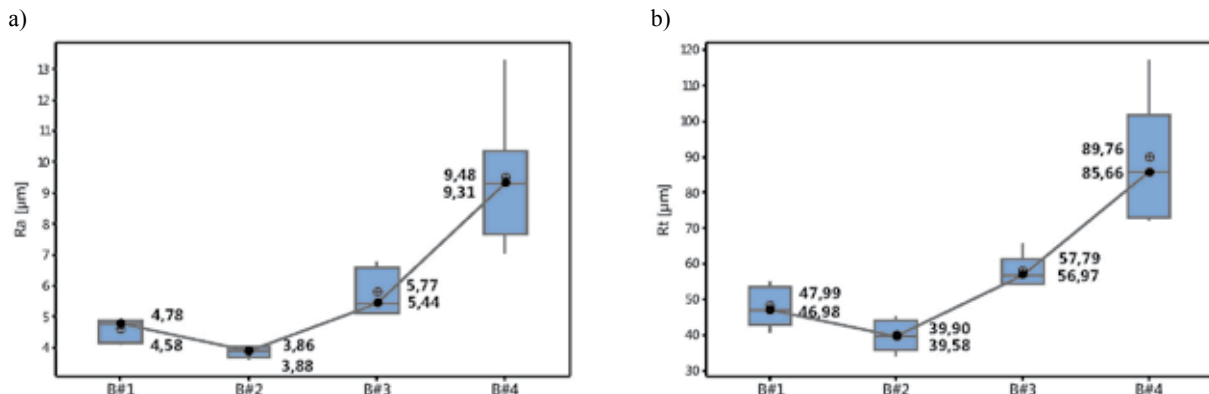
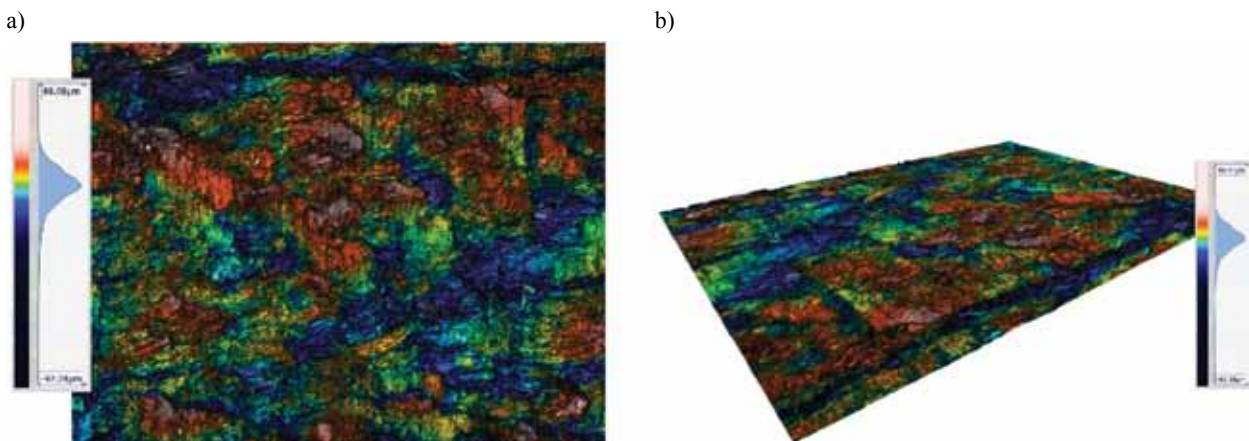
and the ratio of maximum peak height S_p (40.27–42.06 μm) to maximum pit depth S_v (48.92–74.41 μm) changed from the balance between peaks and valleys to a distinct increase in the participation of valleys (Fig. 8). The spreads of the results in this case for both Ra and Rt were on a high level. Additionally, one outlier value was observed caused by a local scratch on the material.

In parts that were tested in the case called Sample #2, four various areas (B#1–B#4) after burnishing were defined. In most cases (B#1), based on median, Ra and

Rt parameters decrease about 2 μm and 20 μm compared with initial turned samples, respectively (Table 5). Higher values of loading force (50 N) did not cause a significant deterioration of the average roughness parameters (B#1 – B#3). On the other hand, areas with the worst surface condition (B#4) were identified, where the total height of profile (Rt) reached about 117 μm with an mean Ra of 89.76 μm (Fig. 9), and for 3D measurements, maximum height (S_z) parameter were in the range of 141.25–152.24 μm (Fig. 10).

Table 5. Roughness parameters of the parts burnished with the loading force of 50 N (Sample#2)

| | B#1 | | B#2 | | B#3 | | B#4 | |
|--------|----------------------|----------------------|----------------------|----------------------|----------------------|----------------------|----------------------|----------------------|
| | Ra [μm] | Rt [μm] | Ra [μm] | Rt [μm] | Ra [μm] | Rt [μm] | Ra [μm] | Rt [μm] |
| Mean | 4.58 | 47.99 | 3.86 | 39.90 | 5.77 | 57.79 | 9.48 | 89.76 |
| Median | 4.78 | 46.98 | 3.88 | 39.58 | 5.44 | 56.97 | 9.31 | 85.66 |
| Q1 | 4.18 | 42.96 | 3.71 | 35.78 | 5.14 | 54.58 | 7.66 | 73.07 |
| Q3 | 4.87 | 53.52 | 4.01 | 44.20 | 6.57 | 61.41 | 10.36 | 101.60 |
| Max | 4.88 | 54.95 | 4.05 | 45.38 | 6.79 | 65.72 | 13.27 | 116.99 |
| Min | 4.10 | 40.98 | 3.64 | 34.01 | 5.07 | 54.34 | 7.05 | 72.33 |

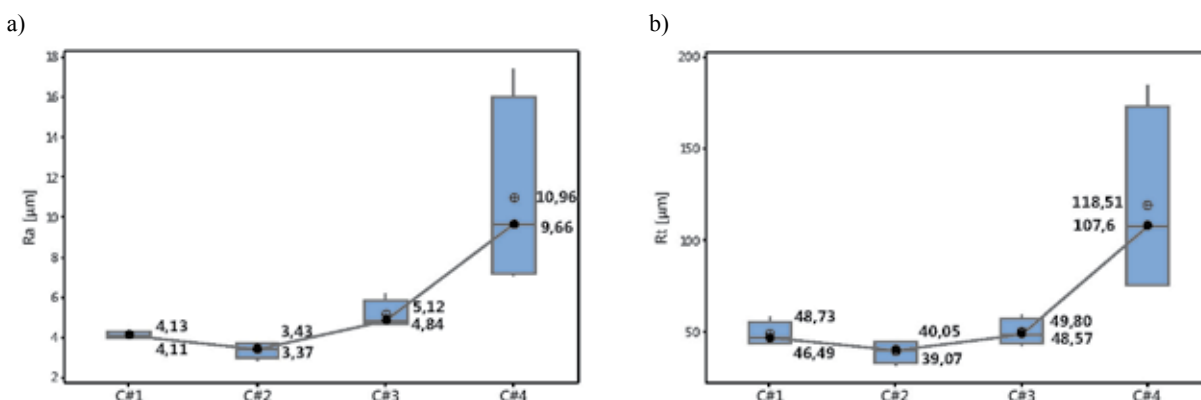
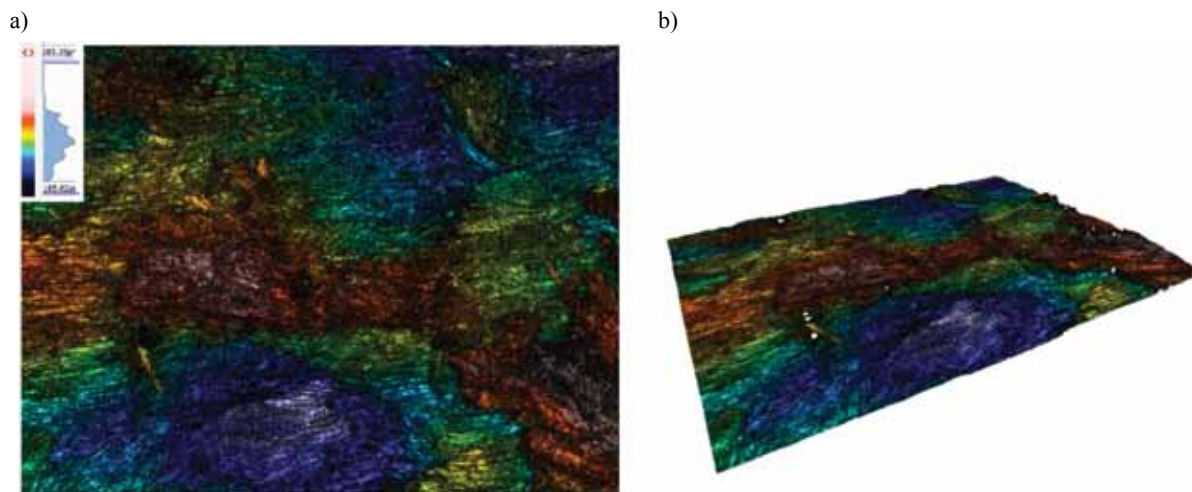
**Fig. 9. The centre and spread of a Ra (a) and Rt (b) parameters of the profile of the parts burnished with the loading force of 50 N (Sample#2) (the box plot presents: the mean, the median, the interquartile range box and the range of the data)****Fig. 10. Surface topography 2D (a) and 3D (b) view**

For Sample#3, five areas were specified based on the surface condition after burnishing. In the C#2 area, the best surface condition were observed, and C#1 and C#3 areas were characterized by the highest contribution in the total machined surface (Table 6). The arithmetical mean height (Ra) raised 2.85 μm with the interquartile spread of 0.72 μm (C#2). The mean and median of the Ra for most surfaces were in the range of 4.11 μm –5.12 μm , and the quartile values indicated a relatively small dispersion (C#1 and C#3) (Fig. 11a). The values of total height of profile (Rt) for C#1, C#2 and C#3 were stable

in the range of 31.01 μm –59.66 μm (Fig. 11b). Finally, for C#4 area, the onset of deterioration of the roughness parameters occurs until the complete destruction of the surface in C#5. The total height of profile (Rt) for C#4 has reached 184.24 μm at 10.96 μm mean arithmetical mean height (Ra). The beginning of the deterioration of the surface condition led to large spread of the roughness parameters obtained. In complete destruction of the surface in C#5, the high peaks and valleys were predominant, and maximum height (Sz) values reached even up to 964.50 μm (Fig. 12).

Table 6. Roughness parameters of the parts burnished with the loading force of 70 N (Sample#3)

| | C#1 | | C#2 | | C#3 | | C#4 | |
|--------|----------------------|----------------------|----------------------|----------------------|----------------------|----------------------|----------------------|----------------------|
| | Ra [μm] | Rt [μm] | Ra [μm] | Rt [μm] | Ra [μm] | Rt [μm] | Ra [μm] | Rt [μm] |
| Mean | 4.13 | 48.73 | 3.37 | 39.07 | 5.12 | 49.80 | 10.96 | 118.51 |
| Median | 4.11 | 46.49 | 3.43 | 40.05 | 4.84 | 48.57 | 9.66 | 107.60 |
| Q1 | 3.97 | 44.12 | 2.98 | 32.82 | 4.67 | 43.74 | 7.18 | 75.27 |
| Q3 | 4.29 | 55.58 | 3.70 | 44.33 | 5.85 | 57.09 | 16.03 | 172.67 |
| Max | 4.35 | 58.35 | 3.78 | 45.16 | 6.19 | 59.66 | 17.43 | 184.24 |
| Min | 3.94 | 43.58 | 2.85 | 31.01 | 4.61 | 42.39 | 7.08 | 74.61 |

**Fig. 11. The centre and spread of a Ra (a) and Rt (b) parameters of the profile of the parts burnished with the loading force of 70 N (Sample#3) (the box plot presents: the mean, the median, the interquartile range box and the range of the data)****Fig. 12. Surface topography 2D (a) and 3D (b) view**

The analysed surfaces were in the form of a plateau with smooth peaks and a concentration of the material near the tops of the profile, which were represented by mean negative skewness R_{sk} in the range of -1.27 – -0.64 (Table 7). The exceptions were C#4 samples with an identified and noticeable beginning of the damaging process of the surface during burnishing when the R_{sk} parameter reached even the value of 2.47. The mean kurtoses (R_{ku}) for all samples were 4.86–7.80, which

indicates the presence of the sharp structure of the profile typical for wooden material after the burnishing process. As can be seen, some of the R_{ku} parameters exceeded 10, which indicates the existence of extremely sharp deep valleys forming the texture of the selected workpieces.

Based on material ratio curve parameters such as R_k (core roughness depth), R_{pk} (reduced peak height) and R_{vk} (reduced valley depth), the above findings on the occurrence of the plateau structure with deep valleys

Table 7. Rsk and Rku roughness parameters of the parts under investigation

| | C#1 | | C#2 | | C#3 | | C#4 | |
|--------|-------|-------|-------|------|-------|------|-------|-------|
| | Rsk | Rku | Rsk | Rku | Rsk | Rku | Rsk | Rku |
| Median | -1.28 | 7.17 | -1.17 | 7.18 | -0.69 | 4.85 | 0.15 | 5.07 |
| Mean | -1.27 | 7.80 | -1.12 | 6.87 | -0.74 | 5.20 | 0.50 | 7.60 |
| Max | -0.80 | 11.92 | -0.70 | 8.36 | -0.19 | 6.72 | 2.47 | 16.09 |
| Min | -1.74 | 4.93 | -1.44 | 4.74 | -1.39 | 4.36 | -0.75 | 4.16 |

| | B#1 | | B#2 | | B#3 | | B#4 | |
|--------|-------|------|-------|------|-------|------|-------|-------|
| | Rsk | Rku | Rsk | Rku | Rsk | Rku | Rsk | Rku |
| Median | -0.86 | 5.13 | -0.77 | 4.79 | -0.60 | 5.15 | -0.66 | 4.25 |
| Mean | -0.73 | 5.31 | -0.69 | 5.05 | -0.78 | 5.70 | -0.87 | 5.60 |
| Max | -0.22 | 6.96 | 0.01 | 7.28 | 0.30 | 8.98 | -0.08 | 10.93 |
| Min | -1.33 | 4.29 | -1.01 | 3.68 | -1.77 | 3.44 | -1.89 | 2.90 |

| | A#1 | | A#2 | |
|--------|-------|------|-------|------|
| | Rsk | Rku | Rsk | Rku |
| Median | -0.68 | 4.57 | -0.71 | 4.21 |
| Mean | -0.64 | 4.86 | -0.77 | 5.05 |
| Max | 0.04 | 9.10 | -0.19 | 9.25 |
| Min | -1.26 | 3.08 | -1.92 | 3.00 |

after burnishing can be confirmed (Table 8). The reduced valley depths (Rvk) were 1.8–2.3 times higher than the corresponding reduced peak heights (Rpk). Similarly to Rsk, only in the case of samples C#4, were the obtained results different (Rpk and Rvk were approximately on the same level).

Table 8. Material ratio curve parameters of the part samples

| | Rk [μm] | Rpk [μm] | Rvk [μm] |
|-----|----------------------|-----------------------|-----------------------|
| A#1 | 13.36 | 5.11 | 9.68 |
| A#2 | 21.56 | 8.44 | 18.61 |
| B#1 | 12.47 | 5.83 | 10.50 |
| B#2 | 11.40 | 4.47 | 8.22 |
| B#3 | 15.45 | 6.69 | 13.63 |
| B#4 | 25.04 | 10.45 | 24.54 |
| C#1 | 11.18 | 4.55 | 10.34 |
| C#2 | 8.84 | 4.20 | 8.54 |
| C#3 | 13.53 | 6.66 | 13.11 |
| C#4 | 29.93 | 22.90 | 25.64 |

Conclusions

The geometrical, dimensional, and surface quality of solid wood workpieces is a crucial factor, which influences further processes, such as painting, coating, etc. Shaping processes like turning or milling enables one to obtain sufficient dimensional accuracy; however, surface quality is unsatisfactory. Burnishing processes where simultaneous application of load, heat, and friction between the tool and machined surface were performed, which made it possible to clearly improve the state of the surface layer. The arithmetical mean height (Ra) for parts burnished reached even the value of 2.85 μm with a low dispersion of the results. As can be seen from the presented research, the important limiting factors are the heterogeneous wood structure and loading force. The excessive growth of the burnishing force in connection with the changing hardness of the machined wood may lead to a significant deterioration of the wooden layer. On the other hand, bulk densification of the sawn timber clearly limits the consumption of varnishes and paints during the final processes of such products, e.g., balusters and mouldings.



References

1. Aguilera A., Munoz H.: Surface roughness and cutting power on Blackwood and Redwood planing. *Maderas: Cienc. tecnol.*, 2011, 13(1), pp. 19–28.
2. Hernández R.F., Cool J.: Effects of cutting parameters on surface quality of paper birch wood machined across the grain with two planing techniques. *Holz Roh Werkst*, 2008, 66, pp. 147–154.
3. Kilic M., Hiziroglu S., Burdurlu E.: Effect of machining on surface roughness of wood. *Building and Environment*, 2006, 41, pp. 1074–1078.
4. Orłowski K.A., Walichnowski A.: Analiza ekonomiczna produkcji warstw licowych podłóg klejonych warstwowo. *Drewno. Pr. Nauk. Donies. Komunik*, 2013, 56(189), pp. 115–126. DOI: 10.12841/wood.1644-3985.022.08
5. Sandberg D., Kutnar A., Mantanis G.: Wood modification technologies – a review. *iForest*, 2017, 10, pp. 895–908. DOI: 10.3832/ifor2380-010
6. Babic M., Kocovic V., Vukelic D., Mihajlovic G., Eric M., Tadic B.: Investigation of ball burnishing processing on mechanical characteristics of wooden elements. *Proceedings of the Institution of Mechanical Engineers, Part C: Journal of Mechanical Engineering Science*, 2017, 231(1), pp. 120–127. DOI: 10.1177/0954406216641711
7. Neyses B, Hagman O, Nilsson A: Development of a continuous wood surface densification process: the roller pressing technique. *Proceedings of the “59th International Convention of Society of Wood Science and Technology. Forest Resource and Products: Moving Toward a Sustainable Future” (LeVan-Green S ed)*, 2016, pp. 17–24.
8. Sadatnezhad SH, Khazaeian A, Sandberg D, Tabarsa T.: Continuous surface densification of wood: a new concept for large-scale industrial processing. *BioResources*, 2017, 12 (2), pp. 3122–3132.
9. Przybylski W.: Smoothing of wood surface by burnishing. *Proceed. of the 16th International Wood Machining Seminar IWMS16*, 2003, pp. 562–567.
10. Orłowski K.A., Javorek J., Lalik L., Przybylski W.: Badania procesu nagniatania tocznego drewna świerkowego. *Mechanik*, 2014, 87(11CD), pp. 201–210.
11. Raatz C., Sanding C: Smoothing of wood and wood based material. In: *14th international wood machining seminar*. 1999, p. 83–87.
12. Sanding C., Raatz C.: Smoothing of profiles with friction tools. In: *Int. Conferences “Production Technologies”*, Hannover, pp. 83–188.
13. Rautkari L, Properzi M, Pichelin F, Hughes M: Surface modification of wood using friction. *Wood Science and Technology*, 2009, 43(3–4), pp: 291–299. DOI: 10.1007/s00226-008-0227-0.
14. Gurau L., Irle M.: Surface roughness evaluation methods for wood products: A review. *Curr Forestry Rep*, 2017, 3(2), pp. 119–131. DOI: 10.1007/s40725-017-0053-4.
15. Sensofar: <http://www.sensofar.com/metrology/sneox/> [Accessed 27 February 2019].
16. ISO: *Geometrical product specifications (GPS) – Acceptance and reverification tests for coordinate measuring machines (CMM) – Part 2: CMMs used for measuring linear dimensions*. [Online]. ISO 10360-2:2009. Available from: <https://www.pkn.pl/>

